Int. J. Heat Mass Transfer. Vol. 20, pp. 855–866. Pergamon Press 1977. Printed in Great Britain

DISPERSED FLOW HEAT TRANSFER

E. N. GANIĆ and W. M. ROHSENOW
Heat Transfer Laboratory, Massachusetts Institute of Technology, Cambridge, MA 02139, U.S.A.

(*Received* 29 *July* 1976 *and in revised form* 3 *November* 1976)

Abstract—An experimental and theoretical analysis of the dispersed flow heat transfer has been performed. The transient experimental technique included a long tubular preheater section for creating a dispersed flow and a short tubular transient test section for collecting the heat-transfer data (heat flux vs wall superheat data). Liquid nitrogen was used as a test fluid. The mass velocities varied from 80 to 300 kg/s m^2.

The theoretical study included: the analysis of the structure of a dispersed flow (the analysis of a drop size and drop size distribution); the analysis of the deposition motion of liquid drops (the migration of drops toward the wall); the analysis of the possible successive states of drop-wall interaction, and heat transfer to a drop deposited on the heated wall.

Based on the above analyses the expression for the heat flux from the wall to dispersed flow has been developed and it has given good agreement with the experimental data.

NOMENCLATURE

a, drop diameter [μm];
$\bar{a}$, mean drop diameter [μm];
a_c, deposition diameter [μm];
A, surface; heat-transfer area of the transient test piece, equation (2) [m^2];
C, correction factor, equations (6) and (26);
C_p, specific heat [J/kg K];
D, tube diameter [m];
f, cumulative (deposition) factor;
f_g, friction factor ($f_g = 0.0791/Re^{0.25}$);
g, gravitational acceleration [m/s^2];
h, heat-transfer coefficient [10], equation (10) [W/m^2 K];
H_{lg}, latent heat of evaporation [J/kg];
k, thermal conductivity [W/m K];
F, gray body factor, equation (23);
m, mass of drop [kg];
M, mass flux of liquid drops [kg/m^2 h];
N, drop deposition flux [No. drops/m^2 h];
$P(a)$, drop size distribution faction [m^{-1}];
Pr, Prandtl number, $P_r = C_p\mu/k$;
q/A, heat flux [W/m^2];
Q, heat transferred to single drop [J];
Re, flow Reynolds number, $Re = GxD/\mu_g\alpha$;
S, slip ratio, $S = V_g/V_l$;
t, time [ms], [s], [min] or [h];
T, temperature [K];
$T_{\min}$, minimum film boiling temperature [K];
u_0, initial drop velocity in the flow direction, equation (12) [m/h];
U_0, vapor velocity ($U_0 = V_g$) [m/h];
U, local vapor velocity [m/h];
U^*, friction velocity [$U^* = U_0(f_g/2)^{1/2}$] [m/h];
v_0, drop deposition velocity ($v_0 = \kappa U^*$) [m/h];
V, volume of the transient test piece, equation (2) [m^3];
V_g, vapor velocity [m/h];
V_l, liquid velocity [m/h];
We, Weber number, equation (3);
x, axial distance, equations (9) and (10) [m];
x, vapor quality;
y, radial distance [m] or [μm].

Greek symbols

α, void fraction;
δ, boundary-layer thickness [m] or [μm];
γ, weight density, equations (5) and (6) in [kg/m^3];
ε, effectiveness of evaporation, equation (16);
κ, constant, equation (13);
μ, viscosity [N/s m^2];
ρ, density [kg/m^3];
σ, Stefan–Boltzmann constant [W/m^2 K^4];
σ, surface tension [N/m].

Subscripts

c, contact;
d, drop;
g, vapor (gas);
l, liquid;
min, minimum;
m, maximum;
mp, most probable;
r, radiation;
sat, saturation;
v, vapor;
w, wall (surface);
wl, wall–liquid;
wv, wall–vapor.

1. INTRODUCTION

DISPERSED flow heat transfer (post dryout heat transfer) has come to be important in recent years due to advancements in various technologies, such as in cryogenics, materials, rocketry, steam generators, and especially in design and safety analysis of nuclear reactors.

Large discrepancies exist among predictions of heat-transfer coefficients in the post dryout region between the correlations and experimental data [1]. Almost all of these correlations are modifications of the well-known Dittus–Boelter type relationship [2] for single-phase flow where various definitions of the "two-phase velocity" and physical properties are used. These correlations are listed in Table 1 of reference [3]. They generally predict a heat-transfer coefficient based on the temperature difference between wall and saturation. As mentioned by Groeneveld [3] they are simple to use but have a limited range of validity and should not be extrapolated outside the recommended range.

Several M.I.T. reports [4–7] deal with a theoretical model for the prediction of the post dryout wall temperature. It was assumed that heat transfer takes place in steps: (a) from the heated wall to the vapor and then from the vapor to the drops; (b) from the heated wall to liquid drops. A similar model was independently developed by Bennett [8]. In these models all parameters (drop size, vapor velocity, liquid velocity, void traction, slip, etc.) are initially evaluated at the dryout location. The heated channel is subdivided axially. The axial gradients in drop diameter, vapor quality, vapor velocity, and liquid velocity are calculated at each node. The vapor superheat is evaluated from a heat balance at each node. The conditions at the downstream nodes are found by step by step integration along the heated channel. The wall temperature is then calculated at each node using superheated vapor heat-transfer correlations [3].

The post dryout heat transfer includes the transition and the film boiling mechanisms of heat transfer. The transition region is related to the lower wall superheat where the heated surface is wetted intermittently by liquid drops and nucleate and film boiling exist side-by-side. In the high wall superheat region, stable film boiling exists and the heated surface is almost dry as discussed later in the text.

In the post dryout heat-transfer the heated surface is cooled by convection to the vapor component of the flow, by evaporation of the liquid drops deposited on the heated wall and by radiation between the wall and dispersed flow. The work by Iloeje *et al.* [9] and Plumer *et al.* [7] approached the analysis of the heat-transfer in post dryout region from the phenomenological point of view. They extended work by Forslund [5] and Hynek [6] and obtained the experimental data in the film boiling region. Their results stimulated this present study.

The objectives of this work include the experimental and theoretical study of the dispersed flow heat transfer. The experimental work includes application of the transient experimental technique. Obtained experimental data are presented in the boiling curve form (i.e. heat flux vs wall superheat for a constant mass flux and vapor quality) covering both the transition and the film boiling region. The theoretical work includes:

(1) Analysis of the structure of the fully-developed dispersed flow. Utilization of the relations for calculation of the maximum drop size, mean drop size and drop size distribution.
(2) Application of the drop deposition model, developed by the authors [10, 11] for predicting the drop deposition flux (the amount of liquid phase in form of drops deposited on the heated wall per unit surface and unit time).
(3) Characterization of the possible successive states of the drop-wall interaction and selection of an empirical relation for the heat transfer to single drop on the heated wall.
(4) Derivation of the relation for the heat flux to dispersed flow which covers both the transition boiling region and the film boiling region, applying results from (1), (2) and (3).

2. EXPERIMENTAL PROGRAM

2.1. *Apparatus*

The loop diagram for the experimental apparatus is given in Fig. 1. It is a once through system employing liquid nitrogen as the test fluid. It was constructed to allow for both a steady-state and transient test runs, but the results analyzed here were obtained in the transient section.

The steady-state test section, a uniformly electrically heated 2.44 m long Inconel 600 tube 12.7 mm O.D. by 10.16 mm I.D., operates as a preheater for the transient test section. In this manner a two-phase flow mixture with a particular vapor quality and mass flux can be supplied to the transient section. The transient test section, Fig. 2, consists of 25.4 mm long tube 10.16 mm I.D. by 25.4 mm O.D. supported and encased to be independently heated with steam supplied at a temperature of 373–400 K. The transient test piece is insulated from the supporting structure by micarta insulators (thermal conductivity of 0.396 W/m K). Three thermocouple holes 1.07 mm in diameter were drilled radially into the test piece to a depth of 0.8 mm from the inside radius [7]. The holes were spaced at three axial positions along the test piece with each hole circumferentially spaced 120° apart. The thermocouples were coated with a conductivity gel and their leads were excited from the steam jacket through conex glands, to the recording devices. Further discussion of the apparatus and the instrumentation for monitoring of the test loop operations and data acquisitions from the transient test section can be found in [7] and [9]. In all cases copper–constantan thermocouples were utilized as the temperature sensing device.

2.2. *Experimental method*

The following sequence of operations was carried out for obtaining dispersed flow heat-transfer data. The steam supply to the transient section was turned on which allowed the test piece to reach an initial temperature of 373–400 K. Liquid nitrogen at 689×10^3 N/m^2 was allowed to flow through two heat exchangers that cool it down sufficiently that it remains liquid as it passes through the flow control valve. The subcooling was achieved by bleeding part of the main

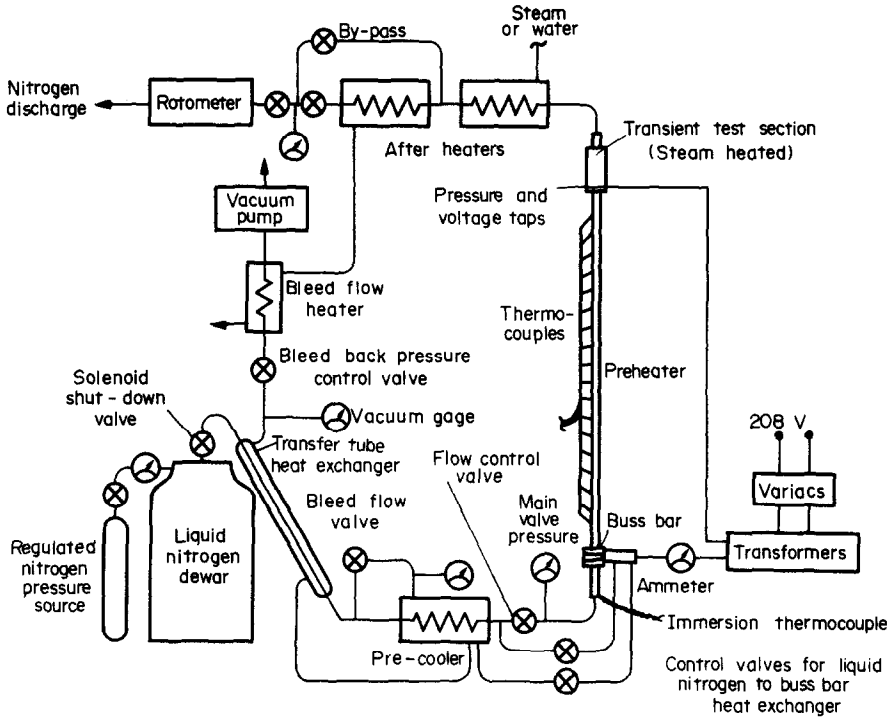

FIG. 1. Nitrogen test loop.

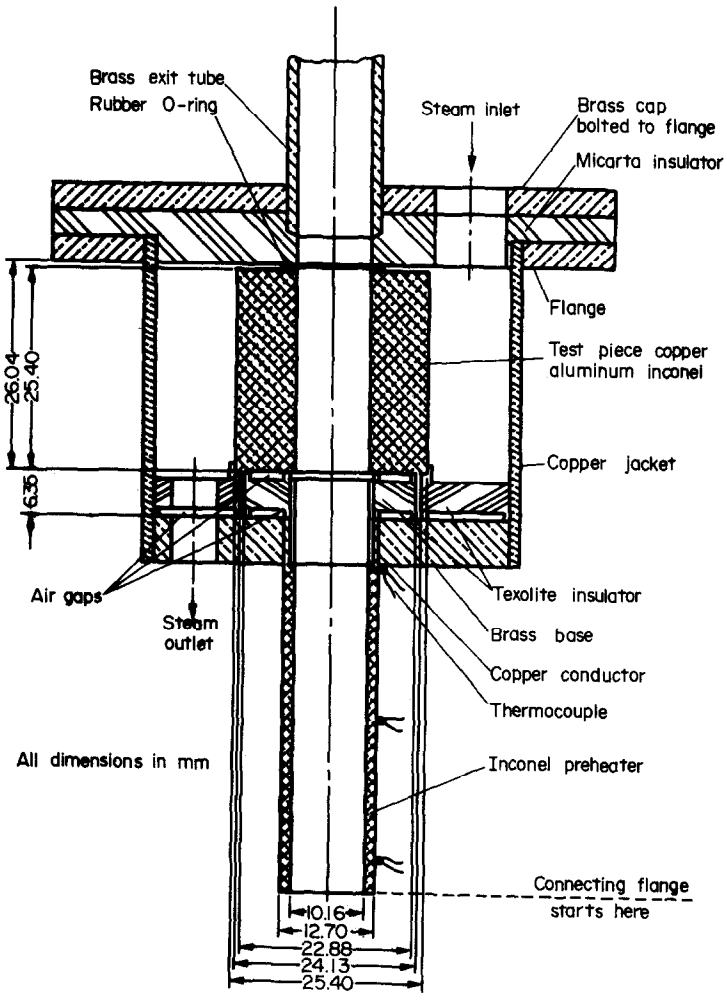

FIG. 2. Transient test section design.

flow into a vacuum line, which forms the outer part of the two concentric-tube heat exchangers. The nitrogen subcooled 2–3 K was initiated into the preheater at about 140×10^3 N/m^2. When the preheater thermocouples registered a temperature near the saturation temperature of the liquid, power was applied to the preheater. The flow rate and power were adjusted to give the desired value of mass flux and exit quality to the transient section for the particular run. When the steady state was achieved in the preheater the transient was initiated by closing off the steam flow to the transient section. The temperature transient was recorded following the data flow diagram in Fig. 7 [7]. Because of the nature of the test, all regimes of boiling existed on the test piece during the transient. A run was terminated when nucleate boiling was re-established. Since the test piece was short, it was possible to assume that the quality variation with distance and time was negligible.

The nitrogen, before passing through the flowmeters (Fig. 1), goes through one or two concentric-tube heat exchangers which serve to heat up the nitrogen to roughly room temperature. The steam or water that flows through the outer part of these heat exchangers also flows through another heat exchanger that heats up the vacuum line so that the vacuum pump does not freeze up.

2.3. *Data deduction*

The three thermocouple outputs, at the three axial positions, in the transient test piece, gave essentially the same temperature–time history

$$T = T(t). \tag{1}$$

Figure 3 shows a typical temperature–time history curve with all regimes of boiling existing.

Considering the transient test piece as a lumped heat source (no internal temperature gradients), the heat flux to the fluid during quenching is given as

$$q/A = \frac{V}{A}\rho C_p \frac{\mathrm{d}T}{\mathrm{d}t}. \tag{2}$$

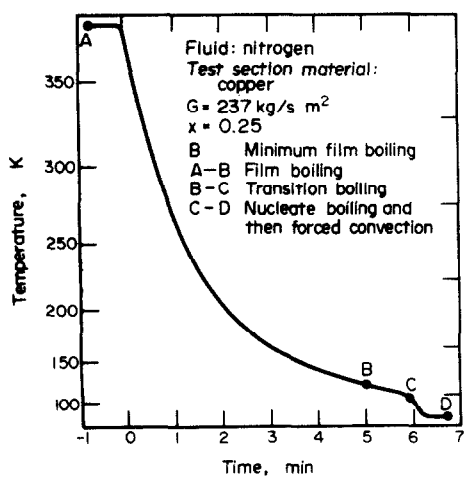

FIG. 3. Temperature–time history.

The Biot number was calculated to be 0.01, 0.018 and 0.24 for the copper, aluminum and inconel test, respectively [9, 7] and therefore the assumption of the lumped heat source is justified. The characteristic dimension L on which Biot number was based, was obtained by dividing the volume of the test piece by its heat-transfer area.

The data for the heat flux to the two-phase mixture, for the particular quality and mass flux, where obtained by introducing the temperature–time data (equation 1) into equation (2).

Figures 8–17 show the heat flux data obtained by the authors. Appendix II-1 of [10] gives the estimate of the heat losses from the transient test section.

3. THEORETICAL WORK

3.1. *Structure of dispersed flow*

The distribution of mass of liquid phase in a dispersed flow is important to the heat-transfer and pressure-drop characteristics of the flow. Small liquid drops dispersed in a gas stream (dispersed flow) usually attain spherical shape due to surface tension. They are uniformly (statistically) mixed independently of their dimensions and the local gas velocity [12].

3.1.1. *Maximum drop diameter.* The most important dimensionless group for determining the stability of a single drop and its maximum size is the Weber number based on the relative velocity and the gas (vapor) density [13],

$$We = \rho_g \frac{(V_g - V_l)^2}{\sigma} a. \tag{3}$$

Critical Weber numbers have been measured experimentally. Isshiki [14] found that $We_c = 6.5$ agreed with his measured water drop diameters which were breaking up in in accelerating stream. This value agrees approximately with Forsulund's [5] value. He found $We_c = 7.5$ for liquid nitrogen drop in its vapor and this value was used in our analysis, so

$$a_m = \frac{7.5\sigma}{\rho_g (V_g - V_l)^2}. \tag{4}$$

3.1.2. *Mean drop diameter.* A wide spectrum of drop diameters is present in dispersed flow. The mean drop diameter can be approximately predicted using simplified Nukiyama–Tanazawa equation.

$$\bar{a} = \frac{1.83}{(V_g - V_l)} \sqrt{\left(\frac{\sigma}{\gamma_l}\right)}. \tag{5}$$

This equation is not dimensionless. The units of the quantities are $\bar{a}$, m; V_g and V_l, m/s; σ, kg/m; γ_l, kg/m^3. Equation (5) has been widely used for predicting the mean drop diameter for atomization with air [13].

For a low mass flux and vapor quality, $\bar{a}$ calculated from equation (5) was larger than experimentally observed average drop diameter in dispersed flow with heat addition [10] where the drop size is influenced not only by aerodynamics and surface forces, but also by evaporation at the drop interface and gravity forces due to relatively low vapor velocity. On the other hand, equation (5) indicates the correct functional relation

between $\bar{a}$ and V_g in dispersed flow (Fig. 3.3 of [10]). It is important to mention that Nukiyama–Tanazawa results [16] show that the mean drop diameter $\bar{a}$ [equation (5)] is not affected by the liquid velocity V_l when the relative velocity $(V_g - V_l)$ was kept constant. Therefore, equation (5) has been applied for predicting the mean drop size in dispersed flow produced by evaporating a liquid in heated tube. Since the vapor velocity V_g in our experiment was considerably less than in Nukiyama–Tanazawa experiment, the correction factor C has been introduced in equation (5),

$$\bar{a} = \frac{1.83C}{(V_g - V_l)}\sqrt{\left(\frac{\sigma}{\gamma_l}\right)}. \tag{6}$$

The values for C, as it will be explained later in the text, are deduced from the experimental data shown in Figs. 8–17.

3.1.3. *Most probable drop diameter.* Experimentally it has been found that a great deal of data satisfied relation [13]

$$a_{mp} = \bar{a}/2. \tag{7}$$

i.e. the average drop diameter is twice as large as the most probable drop diameter. In [17] an empirical relation for a_{mp} has been reported for Freon 12, for specific experimental conditions.

3.1.4. *Drop size distribution.* A large number of drop size distributions have been devised by experiments in order to correlate data. Many authors [13, 18] have used the normal and log-normal distributions which are also in common use for describing crushed particles. In our study the following drop size distribution has been utilized

$$P(a) = 4\frac{a}{\bar{a}^2}\,e^{-2(a/\bar{a})^2} \tag{8}$$

where $\bar{a}$ is the average drop diameter given by equation (6). This type of distribution has been widely used for analyzing and solving mass-transfer and evaporation problems of various dispersed flow systems [19, 20, 21].

The numerical examination of equations (4), (6) and (8) show that drops are smaller for larger $(V_g - V_l)$ which results from higher mass fluxes and vapor qualities. The above equations (4), (6) and (8) are sufficient to characterize the constitution of a dispersed flow, at least for the experimental conditions considered.

3.2. *Deposition of liquid drops in dispersed flow*

The most important phenomenon in the dispersed flow is the deposition motion of drops. By deposition motion, we mean the migration of drops toward the wall. A theoretical analysis of drop deposition from the gas stream on the hot wall has been reported in our previous work [11, 10]. It has been shown [11, 10] that the explanation of the deposition phenomena in the dispersed flow is associated with the theory of the single drop motion inside the boundary layer. Equations of motion of a drop moving in the boundary layers when the main flow in the channel is directed vertically upward are

$$\rho_l\frac{\pi}{6}a^3\frac{d^2x}{dt^2} = \frac{\pi}{16}a^3\rho_g\frac{dU}{dy}\left(\frac{dy}{dt}\right) - 6\pi\mu_g\frac{a}{2}\left(\frac{dx}{dt} - U\right) - (\rho_l - \rho_g)g\frac{\pi}{6}a^3, \tag{9}$$

$$\rho_l\frac{\pi}{6}a^3\frac{d^2y}{dt^2} = -\frac{\pi}{16}a^3\rho_g\frac{dU}{dy}\left(\frac{dx}{dt} - U\right) - 6\pi\mu_g\frac{a}{2}\left(\frac{dy}{dt}\right) + \frac{\pi a^2h^2}{4H_{lg}^2\rho_g}(T_w - T_{sat})^2\frac{a}{\delta}\left(1 - \frac{y}{\delta}\right). \tag{10}$$

Equation (9) was obtained from the equilibrium of forces acting on the drop in the direction of flow (x-direction). Forces acting upwards in the x-direction are taken as positive. Equation (10) was obtained from the equilibrium of forces acting on the drop in the y-direction, y being taken as zero at the wall, increasing positively toward the center line of the channel (tube). The first terms on the RHS of equations (9) and (10) represent the lift forces [11, 10] of the stream flow acting on the periphery of the drop with variation in velocity around the drop, i.e. in the gradient of the stream flow. The second term on the RHS of equations (9) and (10) represent the drag force on the drop. The third term on the RHS of equation (9) represents the gravity and buoyancy forces. The third term on the RHS of equation (10) represents the reaction force on the drop. The reaction force is due to non-uniform drop evaporation inside the boundary layer. Because of the high temperature gradient in the fluid stream close to the hot wall, the velocity of the vapor generated on the drop side facing the wall is higher than the velocity of the vapor generated on the other side. This fact is used in deriving the expression for this force [11, 10]. The tendency of this force is to push the drop away from the wall.

The analytical solution of equations (9) and (10) was obtained [10] assuming the linear velocity profile of the gas stream across the boundary layer:

$$U = U_0\left(\frac{y}{\delta}\right) \tag{11}$$

and applying the following initial conditions:

$$t = 0,\ x = 0,\ \frac{dx}{dt} = \frac{U_0}{S} = u_0, \tag{12}$$

$$t = 0,\ y = \delta,\ \frac{dy}{dt} = \kappa U^* = v_0. \tag{13}$$

Equation (12) assumes that a drop velocity in the flow direction, at $y = \delta$ is approximately independent of drop diameter as experimentally shown in [12]. The velocity of drop crossing the boundary layer [equation (13)] is imparted to the drop by free stream turbulence. The value of $\kappa = 0.15$ [equation (13)] was obtained from the summarized study of deposition of solid particles and liquid drops in two phase mixture by Liu and Ilori [22]. Their summarized results indicated that κ is independent of the particle diameter, in the range from several microns to several hundred microns, for the dispersed flow under consideration [10, 9].

The effects of the wall temperature, drop size, and the initial drop velocities in the parallel and perpendicular directions of flow, on the drop trajectories, are demonstrated on Figs. 4(a–d), respectively.

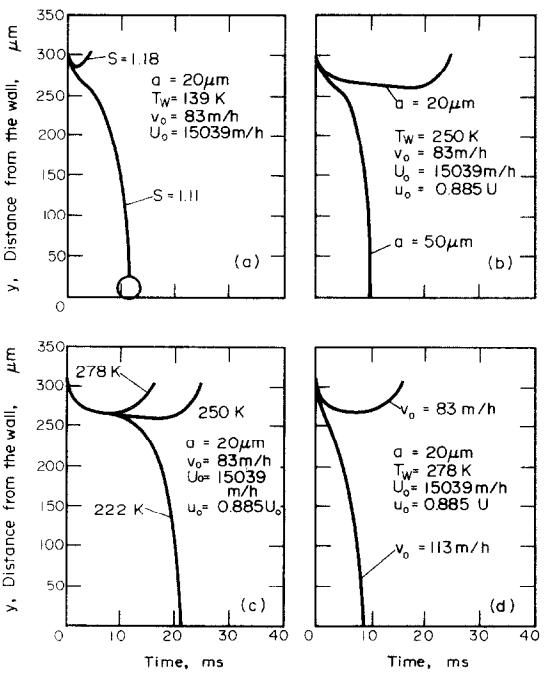

FIG. 4. (a) The effect of slip ratio on the drop trajectory [11]. (b) The effect of drop diameter on the drop trajectory [11]. (c) The effect of wall temperature on the drop trajectory [11]. (d) The effect of drop deposition velocity on the drop trajectory [11].

Prediction of drop trajectories for $a_0 < a \leqslant a_m$ (where a_0 and a_m are minimum and maximum drop diameters respectively, in dispersed flow under consideration) was done by increasing initial drop diameter a_0 step by step and solving the equations (9) and (10) for each value of a, for one particular value of the wall temperature. The summarized results of calculation for $G = 291\,\text{kg/s m}^2$ and $x = 0.49$ are presented on Fig. 5. For example, if the wall temperature was equal to the saturation temperature (no heat addition) then drops with a diameter $a \leqslant 0.81\,\bar{a}$ were returned to the main stream (Fig. 5). The diameter $a = 0.81\,\bar{a}$ for this case is so called the deposition diameter a_c.

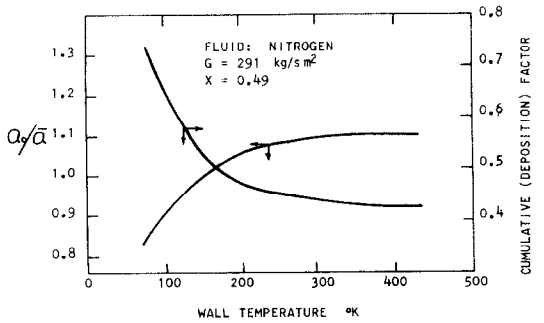

FIG. 5. The effect of wall temperature on the drop deposition diameter and cumulative (deposition) factor.

For the same conditions and the wall temperature of 300 K, $a_c = 1.1\,\bar{a}$ etc. (Fig. 5). The curve in Fig. 5, deposition diameter vs wall temperature, was obtained for the step increase in drop diameter of $\Delta a = 1$ μm. for one particular value of the wall temperature. The step increase in wall temperature was $\Delta T_w = 10$ K. The effect of the wall temperature on the drop deposition is once again demonstrated in Fig. 5.

For the known value of the deposition diameter a_c, and drop size distribution low, equation (8), we define the cumulative (deposition) factor $f(a_c)$ as

$$f(a_c) = \frac{\int_{a_c}^{a_m} a^n P(a)\,da}{\int_0^{a_m} a^n P(a)\,da}. \tag{14}$$

For $n = 3, 2, 1$, $f(a_c)$ represents mass, surface and length cumulative factor, respectively. From equation (14) one can see that $0 \leqslant f(a_c) \leqslant 1$. If the wall temperature increases a_c increases and $f(a_c)$, defined by equation (14), decreases (Fig. 5) since the number of drops deposited on the wall decreases. For any value of a_c, $f(a_c)$ is calculated using equation (8) for $P(a)$. The value of $f(a_c)$ (f in the rest of the text) is used in calculating drop deposition flux as explained later in the text.

In the turbulent core, velocity fluctuations of the main fluid (gas) can not be neglected and the application of equations (9) and (10) is questionable in that region. On the other hand, the drop deposition occurred along trajectories mainly developed in the boundary layer, where equations (9) and (10) are applicable.

3.3. *Heat transfer in dispersed flow*

3.3.1. *Heat transfer to liquid drops.* In dispersed flow liquid drops penetrating the boundary layer collides with the heated wall and cools it by their evaporation. The variables which characterize the drop-wall collision and drop evaporation are numerous [10].

A shape of the liquid drop in contact with solid wall varies with its dimensions. When drop is very small it will keep a spherical shape because of the surface tension effect. In the case of large drop (diameter of the order of several thousands microns or more) it will form disc-shaped liquid film. When a liquid drop touches the wall a contact boundary temperature T_c is immediately established which depends on the initial liquid and wall temperature and on nature of the liquid and wall [9]. Approximately [23],

$$\frac{T_c - T_l}{T_w - T_c} = \left(\frac{(k\rho c_p)_w}{(k\rho c_p)_l}\right)^{1/2}. \tag{15}$$

In spite of the above information, very little is known exactly about thermal behavior of liquid drop deposited on the wall, over a wide range of the wall temperature and the drop impact velocity. In [25], where the experimental study of the dispersed flow drop behavior has been performed using high speed photography, it has been concluded that: (a) As the wall temperature increases, the pictures show fewer and fewer drops touching the wall. The deposition model [equations (9)

and (10) of this study] predicts this phenomenon. (b) Drop-wall contact time decreases as wall temperature increases.

Several other investigators, Parker and Grosh [24], Como *et al.* [26], McGinnis and Holman [27], Forslund and Rohsenow [5], Hynek *et al.* [6], Watchers and Easterling [28], Corman [29], Gaugher [30], Pedersen [31], Toda [32] and Iloeje *et al.* [9] have studied wall-drop interaction. The successive states of drop-wall interaction are shown in Fig. 6. This figure was made after analyzing available experimental results related to the deposition of the drop and its evaporation on the heated wall [25, 26, 33, 9, 32].

Not all possible states of the drop-wall interaction are covered in Fig. 6. Only the most frequently observed states are shown.

Peterson's [31] study of heat transfer to water drops impinging upon a heated surface included variation of the surface temperature from the saturation temperature to 1250 K. These results, effectiveness of evaporation ε, are shown in Fig. 7, together with results of other investigators. The effectiveness of evaporation ε is defined as [31]

$$\varepsilon = \frac{Q}{m[H_{lg} + C_{pl}(T_{sat} - T_l)]}. \tag{16}$$

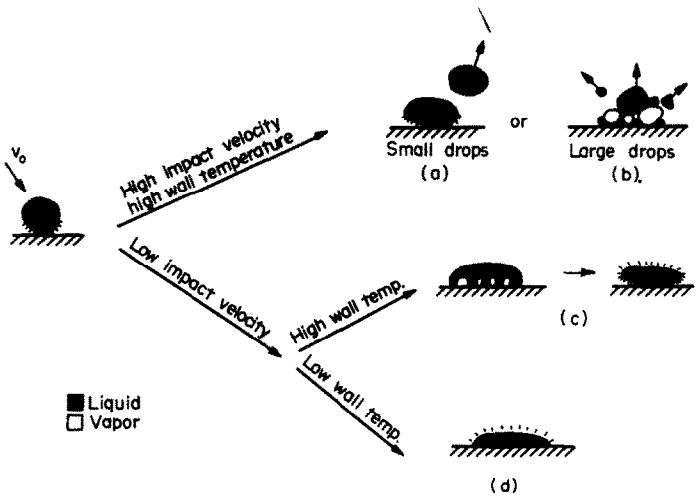

FIG. 6. Successive states of liquid drop-wall interaction.

At the high wall temperature and high impact velocity, tiny drops rebound on the hot wall with little cooling action [25], Fig. 6(a). For the same condition the large drop behavior as shown in Fig. 6(b) where a part of drop is ejected into the main stream by escaping vapor bubbles [26, 33, 9]. In the high temperature region and low impact velocity ($v_0 < 1.8$ m/s) the liquid film formed from the deposited drop is found found to be in a film boiling-like state [Fig. 6(c)] in which a vapor layer is formed between the liquid film and the heated surface [32, 33]. The evaporation of the liquid film on the liquid–vapor layer interface is induced by convective heat transfer through the vapor layer and radiation heat-transfer from the heated wall. The low wall temperature ($T_w < T_{min}$) and low impact velocity case is shown in Fig. 6(d) where the liquid film evaporates from the liquid–vapor interface [32]. At the initial stage of formation of a liquid film on a heated wall, heat is transferred by conduction from the heated wall to the liquid film. When the superheated thermal layer in the liquid film is fully developed evaporation of the liquid film at the liquid–vapor interface takes place. The case 6d has been also rarely reported [32] for the high wall temperature and high impact velocity and due to the very small thickness of the liquid layer (this liquid-layer thickness was studied in [32, 9]) and the very high temperature gradient nucleation is prevented.

In spite of differences [31, 30, 29, 28] in the experimental condition of data in Fig. 7, this figure clearly demonstrates the general effect of the wall (surface) temperature on the evaporation of the deposited drops.

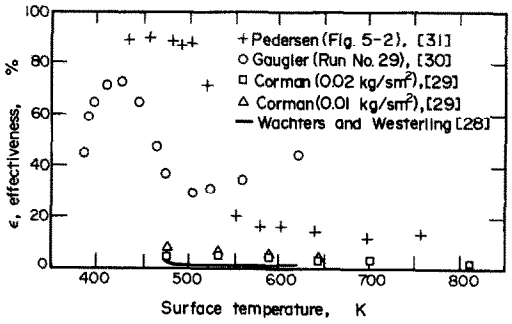

FIG. 7. Effectiveness vs surface temperature.

As can be seen from this figure, the wall cooling due to the direct removal of heat as latent vaporization heat of deposited drops is much less significant at the higher wall temperature.

The wall-drop heat-transfer under stationary vapor-conditions and under flowing vapor conditions (a drop deposited from the vapor stream) are, to a certain extent, different processes. The presence of a vapor and drop velocity parallel to the wall, for example, as in Fig. 6(c), will reduce the vapor layer thickness between

the drop and wall thus increasing the heat transfer through this layer. On the other hand, the presence of the flowing vapor affects the drop deposition much more than it affects the behavior of the already deposited drop on the wall [10].

The list of variables that have a certain influence on the wall-drop heat transfer includes: wall temperature, nature of the fluid, drop impact velocity, nature of the heating wall and coupling of fluid and wall, drop temperature, and surface state of heating wall (micro-roughness, oxidation, etc.).

The "behavior" and the further existence of the liquid film formed from the deposited drop is mostly prescribed by the wall temperature (Figs. 6 and 7). The wall temperature is the most important variable associated with this problem.

The data for water obtained by Pedersen [31] also show that drop impact velocity affects drop heat-transfer in the very high temperature region. In this region drop deposition flux, as later defined, is low; hence, the effect of deposition velocity on the drop-wall heat transfer is small.

Oxide films and crud [9] can reduce the effective liquid drop-surface contact angle and liquid contacting the surface will spread over a wider area, increasing the heat transfer directly to liquid in spite of a high surface thermal resistance layer created by the oxide.

The wall micro-roughness increases the heat transfer to liquid drop. When a liquid drop hits the wall it is possible that it will be dragged along the wall due to its velocity in the flow direction [10]. Therefore, the liquid wets the wall penetrating into the microscopic surface depressions and heats up rapidly, resulting in very fast evaporation [9, 25].

The effect of the drop temperature (drop subcooling) on the drop heat transfer is mentioned in [31]. The drop subcooling increases the heat transfer since it lowers the contact boundary temperature (liquid drop-wall contact boundary temperature) as shown by equation (15).

Decreasing the contact angle (the contact angle between the wall and the liquid drop is measured through the liquid) increases the wettability of the surface, which in turn increases the heat transfer to drop. As shown in Fig. 6, the contact angle is important for the case (d) (low wall temperature, $T_w < T_{min}$) and less important for cases (a), (b) and (c) (high wall temperature) where there is not full contact of the liquid with wall.

The available correlation for Q (heat transferred to deposited single drop evaporating on the wall) [27, 9, 32] are based on the particular values or narrow range of the wall temperature and were not applicable in our study where the wall superheat has been varied largely.

The wall temperature has predominant effect on Q as mentioned. The available experimental data for Q, plotted in Fig. 7, is scattered and appears to have an approximate exponential decay in ε with increase of the wall temperature [31, 25, 26, 30, 29, 28]. Therefore, we assume the following simple expression for ε.

$$\varepsilon = e^{1-(T_w/T_{sat})^m}$$

so

$$Q = \frac{\pi}{6} a^3 \rho_l H_{lg} e^{1-(T_w/T_{sat})^m}. \tag{17}$$

The above expression for ε with $m = 2$ passes through the middle of the scattered data of Fig. 7. This $m = 2$ was used in the analysis.

The mass flux of liquid drops migrating toward the wall, entering the boundary layer, is by definition

$$M = v_0(1-\alpha)\rho_l. \tag{18}$$

The mass flux of liquid drops at the wall [9] is then

$$M_w = v_0(1-\alpha)\rho_l f \tag{19}$$

where f is the mass fraction (cumulative factor) of the drops entering the boundary layer which reach the wall, equation (14).

The drop deposition flux (the number of the drops of equivalent diameter $\bar{a}$, deposited per unit area of the wall unit time) is

$$N = \frac{M_w}{\frac{\pi}{6}\rho_l \bar{a}^3} = \frac{6v_0(1-\alpha)f}{\pi \bar{a}^3} \tag{20}$$

where here $\bar{a}$ = average drop diameter for $a_c < a < a_m$, defined by the following relation

$$\bar{a} = \left(\frac{\int_{a_c}^{a_m} a^3 P(a)\,da}{\int_{a_c}^{a_m} P(a)\,da} \right)^{1/3}$$

and $P(a)$ is given by equation (8).

Applying equation (17) which is based now on $\bar{a}$ defined by the last equation and using $m = 2$, the heat transfer from the wall to liquid drops is

$$(q/A)_d = N \cdot Q = v_0(1-\alpha)\rho_l H_{lg} f\, e^{[1-(T_w/T_{sat})^2]}. \tag{21}$$

The equivalent procedure to the above, in deriving $(q/A)_d$, is presented in Appendix V-1 of [10].

3.3.2. *Heat transfer to vapor.* Heat transfer from the wall in the bulk vapor component of the dispersed flow is given by the McAdams equation, using a vapor flow Reynolds number,

$$(q/A)_v = 0.023 \frac{k_g}{D} Re^{0.8} Pr^{0.4} (T_w - T_{sat}). \tag{22}$$

Fluid properties are calculated at bulk vapor temperature. It was assumed in the above equation that the surface void fraction α_s (percentage of the wall area available for the heat transfer to vapor flow) was equal to unity. The validity of this assumption is presented in Appendix V-2 of [10].

3.3.3. *Radiation heat-transfer.* In dispersed flow the heated wall is also cooled by radiation. It is given as the sum of the radiation heat transfer from the surface to the liquid drops and to the vapor,

$$(q/A)_r = F_{wl}\sigma(T_w^4 - T_{sat}^4) + F_{wv}\sigma(T_w^4 - T_{sat}^4) \tag{23}$$

assuming that the liquid drops and vapor are at the saturation temperature. The evaluation of F_{wl} and F_{wv} was presented in [34] where dispersed system was

assumed gray and diffuse, the absorption and emission of the mixture was incorporated into the network analysis by treating the system as an enclosure filled by a radiating gas and a cloud of liquid drops.

3.3.4. *Total heat-flux.* The total heat-flux from the wall to the dispersed flow is given by the sum of equations (21)–(23),

$$q/A = (q/A)_d + (q/A)_v + (q/A)_r. \quad (24)$$

For nitrogen dispersed flow $(q/A)_r$ was negligible [10] and

$$q/A = v_0(1-\alpha)\rho_l H_{lg} f \, e^{[1-(T_w/T_{sat})^2]} + 0.023\frac{k_g}{D} Re^{0.8} Pr^{0.4}(T_w - T_{sat}). \quad (25)$$

The comparison of equation (25) with the experimental data obtained in this study, for a relatively wide range of mass fluxes and vapor qualities are presented in Figs. 8–17.

4. DISCUSSION

The values of C in equation (6) selected for prediction of the experimental data in Figs. 8–17, satisfy a developed empirical relation:

$$C = 0.4/[(V_g - V_l)D\rho_g/\mu_g]^{0.5} \quad (26)$$

It was discussed in more detail in Appendix V-6 of [37].

In order to find q/A from equation (25), the procedure of calculation is as follows. For given G and x, the value of the slip ratio S, in our study, is calculated using modified Plummer's method as explained in Appendix V-6 of [37]. The predictions in Figs. 8–17 are sensitive on the value of S, especially in the vicinity of and below the minimum film boiling temperature where the heat transfer to liquid drop is high.

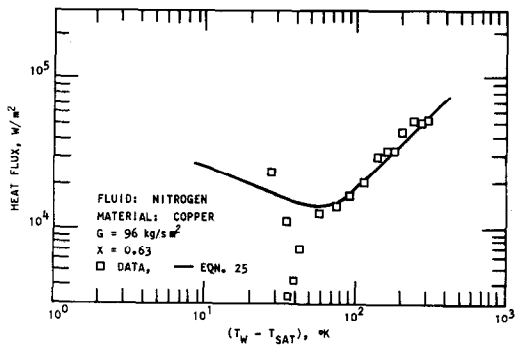

FIG. 8. Heat flux vs wall superheat.

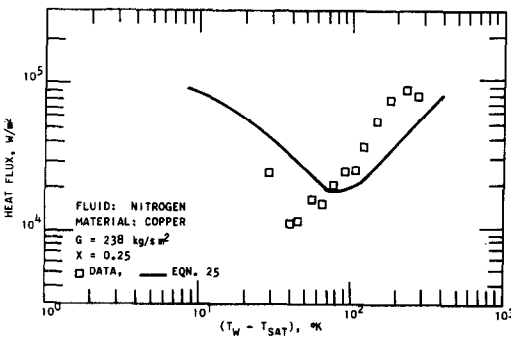

FIG. 9. Heat flux vs wall superheat.

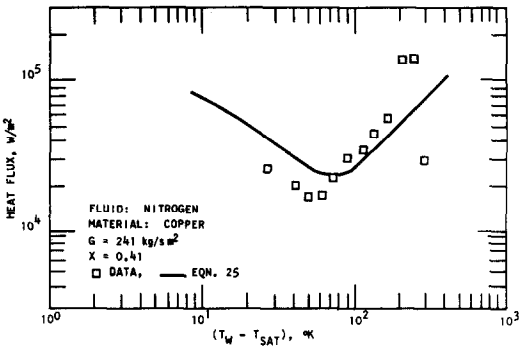

FIG. 10. Heat flux vs wall superheat.

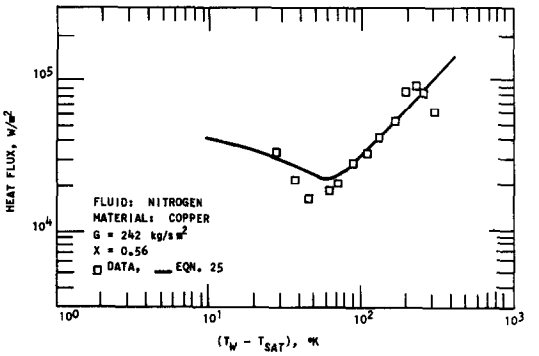

FIG. 11. Heat flux vs wall superheat.

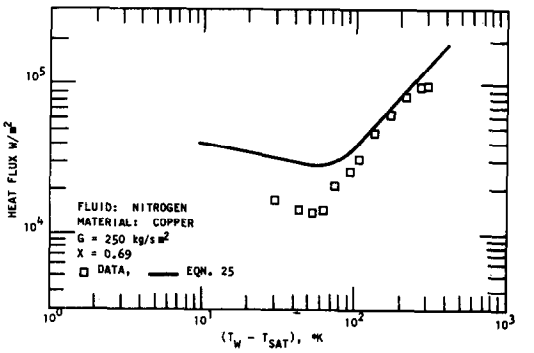

FIG. 12. Heat flux vs wall superheat.

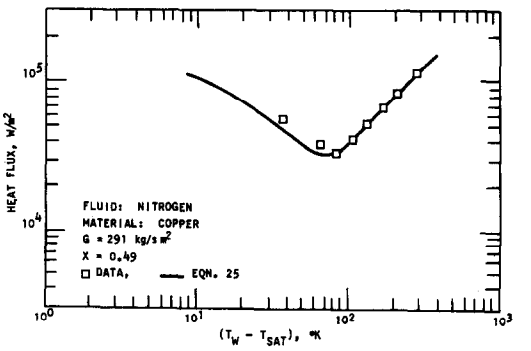

FIG. 13. Heat flux vs wall superheat.

Other correlations for a slip ratio are presented in [35, 36]. The void fraction is then

$$\alpha = \frac{x}{x + \frac{\rho_g}{\rho_l} S(1-x)}$$

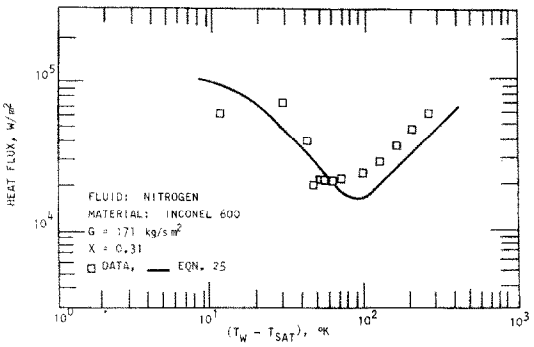

FIG. 14. Heat flux vs wall superheat.

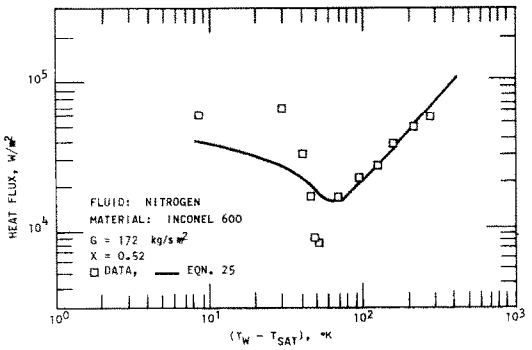

FIG. 15. Heat flux vs wall superheat.

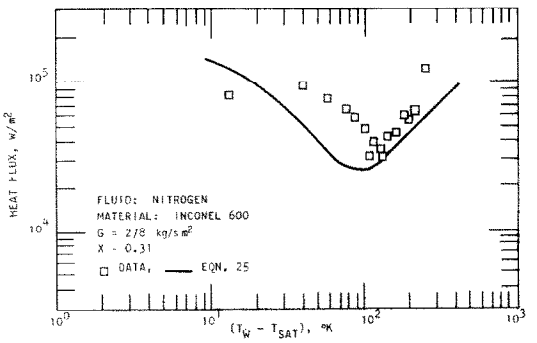

FIG. 16. Heat flux vs wall superheat.

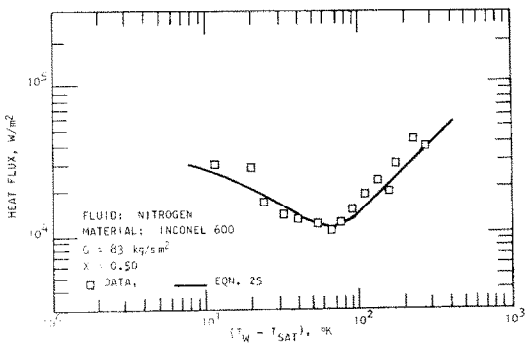

FIG. 17. Heat flux vs wall superheat.

and velocities

$$V_g = \frac{Gx}{\alpha\rho_g}, \quad V_l = \frac{G(1-x)}{\rho_l(1-\alpha)}.$$

Drop deposition velocity:

$$v_0 = 0.15U^* = 0.15\frac{Gx}{\rho_l\alpha}\sqrt{\left(\frac{f_g}{2}\right)}$$

where the friction factor f_g is based on the vapor Reynolds number. The mass cumulative (deposition) factor f, after integration of equation (14), with $m = 3$ is given as

$$f = \left\{\left[\left(\frac{a_c}{\bar{a}}\right)^3 + \frac{3}{4}\left(\frac{a_c}{\bar{a}}\right)\right]\exp\left[-2\left(\frac{a_c}{\bar{a}}\right)^2\right] - \left[\left(\frac{a_m}{\bar{a}}\right)^3 + \frac{3}{4}\left(\frac{a_m}{\bar{a}}\right)\right]\exp\left[-2\left(\frac{a_m}{\bar{a}}\right)^2\right] + \frac{6}{16}\sqrt{(\pi/2)}\left[\operatorname{erf}\left(\sqrt{2}\frac{a_m}{\bar{a}}\right) - \operatorname{erf}\left(\sqrt{2}\frac{a_c}{\bar{a}}\right)\right]\right\} \times \left\{\frac{6}{16}\sqrt{(\pi/2)}\operatorname{erf}\left(\sqrt{2}\frac{a_m}{\bar{a}}\right) - \left[\left(\frac{a_m}{\bar{a}}\right)^3 + \frac{3}{4}\left(\frac{a_m}{\bar{a}}\right)\right]\exp\left[-2\left(\frac{a_m}{\bar{a}}\right)^2\right]\right\}^{-1}.$$

In calculating f, a_m is calculated from equation (4), $\bar{a}$ from equation (6) where values for C are obtained from equation (26). Deposition diameter a_c is obtained from the solution of equations (9) and (10) for specified values of T_w as explained in Section 3.2.

A significant degree of thermal non-equilibrium can exist in a dispersed flow, i.e. a vapor can be superheated. The vapor superheat can be evaluated using Plummer's or Gwoeneveld's [3] models for vapor superheat, obtained from the experimental data. In the experimental data reported in this study (Figs. 8–17), no thermal, non-equilibrium was present as the preheater section was very long and preheater heat flux was low [10].

The transient test section surface for the data in Figs. 8–17 was smooth and free of oxide. Reader is referred to [7] and [9] for the specific experimental evidence about the effects of the oxide and wall roughness on post dryout heat-transfer.

5. CONCLUSIONS

Based on the analysis of the structure of dispersed flow, drop deposition, drop-wall heat-transfer, including also convection to the vapor component of the flow and radiation heat transfer, the relation [equation (24)] for the heat transfer to the dispersed flow was developed. Since $(q/A)_r$ was very small for the nitrogen dispersed flow, equation (25) was used.

Figures 8–17 show that the equation (25) is capable of predicting the experimental data.

The equation (25) represents a well-known boiling curve for specified values of mass flux, vapor quality, and system pressure. It covers a low and high wall superheat dispersed flow heat-transfer, i.e. flow transition boiling and flow film boiling, respectively. The minimum value of q/A [equation (25)] corresponds to the minimum film boiling temperature (the rewet wall superheat).

The effect of the mass flux and vapor quality on q/A, given by equation (25), is as follows:

(a) When the mass flux increases (constant vapor quality assumed) q/A increases and T_{min} increases.

(b) When the vapor quality increases (constant mass flux assumed), $(q/A)_d$ decreases, $(q/A)_n$ increases, and T_{min} decreases. This affects q/A in such a way that q/A increases in the high temperature region (film boiling region) and decreases in the low temperature region (transition boiling region.

These conclusions are experimentally supported, Figs. 8–17.

The effect of the quality on q/A is rather poorly demonstrated at low mass fluxes but is well demonstrated at higher values of mass flux (cf. Figs. 13 and 16).

The additional studies on the average drop size in dispersed flow and mechanism of the heat transfer to a single drop deposited on the wall, are currently under way in our laboratory.

Acknowledgements—This work was supported by a grant from the National Science Foundation. Professors P. Griffith, A. A. Sonin and P. Thullen gave generously of their time to discuss various aspects of this work. Ms. G. E. Kendall and Mr. G. Yoker made valuable suggestions.

REFERENCES

1. D. S. Slaughterbeck, W. E. Vesley, L. J. Ybarrondo, K. G. Condie and R. J. Mattson, Statistical regression analysis of experimental data for flow film boiling heat transfer, ASME Publication 73-HT-20 (1973).
2. J. G. Collier, *Convective Boiling and Condensation.* McGraw-Hill, London (1972).
3. D. C. Groeneveld, Post dryout heat transfer: physical mechanisms and a survey of prediction methods, *Nucl. Engng Design* **32**, 283–294 (1975).
4. W. F. Laverty and W. M. Rohsenow, Film boiling of saturated liquid flowing upward through a heated tube: high vapor quality range, M.I.T. EPL Report No. 9857-32 (1964).
5. R. P. Forslund and W. M. Rohsenow, Thermal non-equilibrium in dispersed flow film boiling in a vertical tube, M.I.T. Report No. 75312-44 (1966).
6. S. J. Hynek, W. M. Rohsenow and A. E. Bergles, Forced convection dispersed flow film boiling, M.I.T. Report No. 70586-63 (1969).
7. D. N. Plummer, O. C. Iloeje, W. M. Rohsenow, P. Griffith and E. N. Ganić, Post critical heat transfer to flowing liquid in a vertical tube, M.I.T. Report No. 72718-91 (1974).
8. A. W. Bennett, G. R. Hewitt, H. A. Kearsey and R. K. F. Keeys, Heat transfer to steam–water mixtures flowing in uniformly heated tubes in which the CHF has been exceeded, AERE-R-5373 (1967).
9. O. C. Iloeje, D. N. Plummer, W. M. Rohsenow and P. Griffith, A study of wall rewet and heat transfer in dispersed vertical flow, M.I.T. Report No. 72718-92 (1974).
10. E. N. Ganić, Post critical heat flux heat transfer, Sc.D. Thesis, M.I.T. (1976).
11. E. N. Ganić and W. M. Rohsenow, On the mechanism of liquid drop deposition in two-phase flow, ASME Meeting, New York City, December (1976).
12. M. Cumo, G. Ferrani and G. E. Farello, A photographic study of two-phase, highly dispersed flows, CNEN-RT/ING (72) 19, pp. 241–268 (1972).
13. G. B. Wallis, *One-Dimensional Two-Phase Flow.* McGraw-Hill, New York (1969).
14. M. Isshiki, Theoretical and experimental study on atomization of liquid drop in high speed gas stream, Report No. 35, Transportation Technical Research Institute, Tokyo, Japan, July (1959).
15. M. E. Deich and G. A. Filippov, *Gas Dynamics of Two-Phase Media* [in Russian]. Energiya, Moskwa (1968).
16. S. Nukiyama and Y. Tanasawa, An experiment on the atomization of liquid by means of an air stream, Reports 1 and 4, *Truns. Japan Soc. Mech. Engrs* **4**(14), 86 (February 1938) and **5**(18), 68 (February 1939).
17. M. Como, G. E. Farello, G. Ferrari and G. Palazzi, On two-phase highly dispersed flows, CNEN-RT/ING (72) 19, pp. 203–217 (1972).
18. S. L. Soo, *Fluid Dynamics of Multiphase Systems.* Blaisdell, Waltham, MA (1967).
19. A. H. Shapiro and A. J. Erickson, On the changing size spectrum of particle clouds undergoing evaporation, combustion, or acceleration, *Trans. Am. Soc. Mech. Engrs* **79C**, 775–788 (1957).
20. H. C. Hottel and McC. Stewart, Space requirement for the combustion of pulverized coal, *Ind. Engng Chem.* **32**, 719–720 (1940).
21. R. P. Probert, The influence of particle size and distribution in the combustion of oil droplets, *Phil. Mag.* **37**, 94–105 (1946).
22. Y. H. Liu and T. W. Ilori, On the theory of aerosol deposition in turbulent pipe flow, Particle Technology Laboratory Publ., No. 210, University of Minnesota (1973).
23. B. B. Mikic, Conduction heat transfer—class notes, Mechanical Engineering Department, M.I.T., Spring (1974).
24. J. D. Parker and R. J. Grosh, Heat transfer to a mist flow, ANL-6291 (1961).
25. M. Cumo and G. E. Farello, Heated wall-droplet interaction for two-phase flow heat transfer in liquid deficient region, CNEN-RT/ING (72) 19, pp. 146–178 (1972).
26. M. Cumo, G. E. Farello and G. Ferrari, Notes on droplet heat transfer, CNEN-RT/ING (72) 19, pp. 180–202 (1972).
27. F. K. McGinnis and J. P. Holman, Individual droplet heat transfer rates for splattering on hot surfaces, *Int. J. Heat Mass Transfer* **12**, 95–108 (1969).
28. L. H. J. Wachters and N. A. J. Westerling, The heat transfer from a hot wall to impinging water drops in the spheroidal state, *Chem. Engng Sci.* **21**, 1047–1056 (1966).
29. J. C. Corman, Water cooling of a thin, high temperature metal strip, Ph.D. Thesis, Carnegie Institute of Technology (1966).
30. R. E. Gaugler, An experimental study of spray cooling of high temperature surfaces, Ph.D. Thesis, Carnegie Institute of Technology (1966).
31. C. O. Pedersen, The dynamics and heat transfer characteristics of water droplets impinging upon a heated surface, Ph.D. Thesis, Carnegie Institute of Technology (1967).
32. S. Toda, A study of mist cooling (2nd Report: Theory of mist cooling and its fundamental experiments) *Heat Transfer—Japanese Res.* **1**(3), 39–307 (1972).
33. S. Nishio and M. Hirata, An experimental study of the dynamic behavior of a liquid drop deposited upon a heated surface. Unpublished Work—private Communication, Department of Mechanical Engineering, University of Tokyo (1975).
34. K. H. Sun, J. M. Gonzalez and C. L. Tien, Calculations of combined radiation and convection heat transfer in rod bundles under emergency cooling conditions, ASME Publication 75-HT-64 (1975).
35. L. S. Tong and J. D. Young, A phenomenological transition and film boiling heat transfer correlation, *Proceedings of the Fifth International Heat Transfer Conference, Tokyo*, Paper B3.9, pp. 120–124 (1974).
36. D. C. Groeneveld, The thermal behavior of a heated surface at and beyond dryout, AECL-4309 (1972).
37. E. N. Ganic and W. M. Rohsenow, Post critical heat flux heat transfer, M.I.T. Report No. 82672-97 (1976).

TRANSFERT THERMIQUE DES ECOULEMENTS DISPERSES

Résumé—On conduit l'étude théorique et expérimentale du transfert thermique d'un écoulement dispersé. Le montage expérimental comprend une longue partie tubulaire de préchauffage pour obtenir un écoulement dispersé et une courte section tubulaire de mesure du transfert thermique (flux pariétal en fonction de la surchauffe de paroi). On utilise l'azote liquide comme fluide d'essai. Les vitesses massiques varient de 80–300 kg/s m^2.

L'étude théorique inclut: l'analyse de la structure de l'écoulement dispersé (distribution de la taille des gouttes); l'analyse du dépot des gouttes (migration des gouttes vers la paroi); l'analyse des états successifs possibles de l'intéraction goutte-paroi et du transfert thermique à une goutte déposée sur la paroi chaude.

On a obtenu à partir des analyses précédentes l'expression du flux thermique entre paroi et écoulement dispersé, laquelle est en accord satisfaisant avec les résultats expérimentaux.

WÄRMEÜBERGANG IN DISPERSIONSSTRÖMUNGEN

Zusammenfassung—Der Wärmeübergang in Dispersionsströmungen wurde experimentell und theoretisch untersucht. Die Versuchsanlage bestand aus einer langen Rohrvorheizstrecke zur Erzeugung der Dispersionsströmung und einer kurzen Rohrmeßstrecke zur Bestimmung der Wärmeübergangs-Daten (Wärmestromdichte und Wandüberhitzung). Als Versuchsfluid wurde flüssiger Stickstoff verwendet. Die Massenstromdichte bewegte sich zwischen 80 und 300 kg/m^2 s.

Im Rahmen der theoretischen Betrachtung wurde die Struktur der Dispersionsströmung (Tropfengröße und Tropfenverteilung), die Absetzbewegung der Flüssigkeitstropfen (Wanderung der Tropfen zur Wand), die möglichen aufeinanderfolgenden Stadien der gegenseitigen Einwirkung von Tropfen und Wand und der Wärmeübergang an Tropfen auf der beheizten Wand untersucht.

Aufgrund dieser Analyse wurde ein Ausdruck für den Wärmestrom von der Wand an die Dispersionsströmung entwickelt, wobei sich eine gute Übereinstimmung mit den Versuchsergebnissen ergab.

ПЕРЕНОС ТЕПЛА В ДИСПЕРСНОМ ПОТОКЕ

Аннотация — Анализируются результаты экспериментальных и теоретических исследований переноса тепла в дисперсном потоке. Экспериментальный стенд состоял из длинной трубчатой секции предварительного нагрева для образования дисперсного течения и короткой трубчатой измерительной секции для снятия данных по теплопереносу (зависимости теплового потока от перегрева стенки). В качестве рабочей жидкости использовался жидкий азот. Массовые скорости изменялись от 80 до 300 кг/сек.м^2.

Теоретическое исследование включало в себя анализ структуры дисперсного потока (анализ размера капли и распределение размеров капли); анализ осаждения капель жидкости (миграция капель по направлению к стенке); анализ возможных последовательных стадий взаимодействия капли со стенкой и переноса тепла по направлению к капле, осаждающейся на нагреваемой стенке.

На основе проведенных вышеуказанных анализов получено выражение для переноса тепла от стенки к дисперсному потоку, которое хорошо согласуется с экспериментальными данными.